Proceedings of the 21st ICSMGE, Vienna, Austria, 14 – 19 June 2026. Pistrol, Adam & Schweiger (eds.)
Published by: ÖGG, Austrian Society for Geomechanics, Salzburg, Austria, ISBN 978-3-9503898-4-5
https://doi.org/10.53243/ICSMGE2026-1977

Liquefaction Potential Assessment and Damage Evaluation in the Gölbaşı Following the Kahramanmaraş Earthquake

İlknur Bozbey, Sadık Oztoprak, Mustafa Kubilay Kelesoglu, Sinan Sargin, **Emirhan Altinok**, Güldem Korkmaz
Department of Civil Engineering, Istanbul University-Cerrahpasa, Istanbul, Türkiye, emirhanaltinok@iuc.edu.tr

Ahmet Kaan Yildirim
Department of Civil Engineering, Istanbul Nisantasi University, Istanbul, Türkiye

Fatma Tugce Cinar Ozkan
Department of Civil Engineering, Kahramanmaras Sutcu Imam University, Kahramanmaras, Türkiye

Cihan Oser, Zulal Akbay Arama
Department of Civil Engineering, Istanbul University-Cerrahpasa, Istanbul, Türkiye

ABSTRACT: In saturated soils, the increase in shear stresses during an earthquake can lead to a sudden loss of rigidity and strength in the soil beneath building foundations. This can result in significant collapses and loss of stability, causing the building to partially or completely lose its functionality. The earthquake that struck the Kahramanmaras region of Türkiye on February 6, 2023, caused widespread casualties and severe structural damage of this nature. Soil liquefaction played a pivotal role in the extent of the destruction in the Gölbaşı district of Adıyaman province, where buildings situated near Gölbaşı Lake exhibited varying levels of foundation damage. The observed settlement and tilt due to liquefaction varied considerably, emphasizing the complex relationship between soil conditions and structural responses. This study aims to evaluate the predictive accuracy of existing liquefaction-induced damage assessment methods by comparing them with actual settlement and tilt data collected during the research. A comprehensive field-testing program was conducted in the area, including a series of Standard Penetration Tests (SPT) and Cone Penetration Tests (CPT). In the first phase, Liquefaction Potential Index (LPI) and Liquefaction Severity Number (LSN) values were calculated based on the SPT and CPT results. In the second phase, the levels of foundation damage due to liquefaction in thirty-four of the investigated buildings were estimated using empirical formulas that are commonly accepted and available in the literature. The predicted damage levels were compared with the actual observed structural and geotechnical damage. The findings of this study offer valuable insights into the reliability and limitations of current liquefaction potential assessment methods and settlement and tilt prediction models, particularly in areas prone to liquefaction.

KEYWORDS: Liquefaction, building settlement, liquefaction potential index, liquefaction severity number.

1 INTRODUCTION

Soil liquefaction is one of the most critical geotechnical hazards during strong earthquakes, as it can lead to sudden loss of strength in saturated, loose sandy or silty deposits. The resulting ground deformations, such as settlement, lateral spreading, and bearing capacity failures, can severely compromise building foundations and cause widespread damage. Past earthquake events in Türkiye have also provided clear evidence of these effects, creating valuable opportunities to document and analyze liquefaction-related damage under real field conditions. Following the 17 August 1999 Adapazarı Earthquake, extensive field investigations provided a significant database for the characterization of liquefied soils and associated foundation failures, making a notable contribution to the international literature (Bray & Stewart, 2000; Bray et al., 2004).

The February 6, 2023 Kahramanmaraş Earthquakes generated valuable new data, particularly in the Gölbaşı district of Adıyaman province, where widespread liquefaction led to varying levels of foundation damage. The severity and manifestation of damage appeared to be influenced not only by the geotechnical properties of the liquefied soils but also by building geometry, alignment, and interaction between adjacent structures, factors that have been extensively examined in recent studies (Moug et al., 2023; Flora et al., 2024; Tonyali et al., 2024; Cetin et al., 2025). Previous investigations following the February 6, 2023 earthquakes have proven that many buildings in the Gölbaşı district of Adıyaman experienced severe liquefaction-induced foundation damage (Bozbey et al., 2024). Dramatically, a large proportion of the damaged buildings were relatively new, with construction completed after 2016. This emphasizes the need to evaluate liquefaction hazards and the risks of settlement and tilt at the design stage. In this context, cumulative liquefaction hazard indices such as the Liquefaction Potential Index (LPI) and the Liquefaction Severity Number (LSN), together with empirical settlement-prediction equations (e.g., Karamitros et al., 2013; Bray & Macedo, 2017; Bullock et al., 2019), provide valuable tools for anticipating the extent of potential damage. The recent disaster has once again highlighted the importance of employing such methods in the design stage to enable effective mitigation measures in regions known to be susceptible to liquefaction.

The objective of this study is to assess the predictive reliability of existing empirical models for liquefaction-induced damage by validating their estimates against field-measured building settlements and tilts. As part of a nationally funded research project (Bozbey et al., 2023), a comprehensive field-testing program was conducted in the area, including a series of Standard Penetration Tests (SPT) and Cone Penetration Tests (CPT). In the first phase, Liquefaction Potential Index (LPI) and Liquefaction Severity Number (LSN) values were calculated based on the SPT and CPT results. In the second phase, the levels of liquefaction-induced foundation damage in thirty four of the studied buildings were estimated using widely adopted empirical formulas developed by Karamitros et al. (2013), Bray & Macedo (2017), and Bullock et al. (2019). The predicted damage levels were compared with the actual observed structural and geotechnical damage.

2 DESCRIPTION OF THE STUDY AREA

Following the 6 February 2023 Kahramanmaras earthquakes, liquefaction-induced settlements were investigated within the context the project in thirty four buildings located in the Gölbaşı district of Adıyaman province. Settlement and tilt measurements were recorded for these structures, forming the basis of a comprehensive field database. To characterize the subsurface profile of the study area and to identify the properties of both liquefiable and non-liquefiable soils, 10 Standard Penetration Tests (SPT) and 14 Cone Penetration Tests (CPT) were conducted. The locations of the investigated buildings and in-situ tests within the study area are presented in Figure 1.

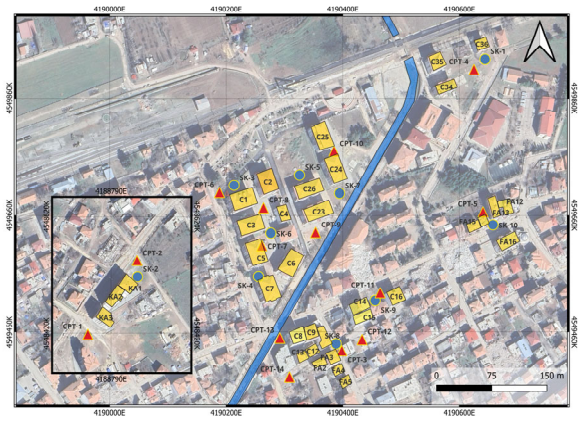

Figure 1. The locations of the investigated buildings and in-situ tests within the study area.

3 DATA AND METHODOLOGY

3.1 *Data Collection and Field Test Measurements*

Field measurements of actual liquefaction-induced building damage were conducted within the first month following the 6 February 2023 Kahramanmaraş earthquakes. A comprehensive database was compiled, containing the geometric properties and post-earthquake damage conditions, settlement, tilt, and structural damage, for a total of 121 buildings in the Gölbaşı district. For the purposes of this study, a subset of 34 buildings was selected from this database. The selection criteria focused on structures exhibiting no structural damage but clear and distinguishable liquefaction-induced settlement and tilt.

Subsequent site investigations were performed to characterize the subsurface conditions in the vicinity of the selected buildings. These investigations included boreholes, Standard Penetration Tests (SPT), Cone Penetration Tests (CPT), Multichannel Analysis of Surface Waves (MASW), and Spatial Autocorrelation (SPAC) tests. Using the boreholes, SPT, and CPT data, the upper 20 m of the soil profile was examined in detail to distinguish liquefiable and non-liquefiable layers. The MASW and SPAC tests provided additional seismic parameters, including shear wave velocity profiles and the depth to bedrock.

The CPTu tests were conducted in accordance with ASTM D3441 using a Dutch-manufactured cone penetrometer with a projected tip area of 10 cm², a friction sleeve surface area of 150 cm², and an advancement rate of 2 cm/s. In addition to cone tip resistance (q_c) and sleeve friction (f_s), pore water pressure (u) was continuously recorded during penetration.

The SPTs were performed during drilling at 1.5 m intervals in accordance with ASTM D1586. Disturbed samples retrieved from the SPTs were subsequently tested in the laboratory for grain-size distribution (sieve analysis), Atterberg limits, and hydrometer analysis. This allowed the characterization of all soil layers in the study area at 1.5 m depth intervals. Based on these results, the upper 20 m generally consisted of clayey sands (SC) with intermittent sand–clay interlayers. The clayey layers were predominantly CL, with only a few boreholes revealing thin CH layers. The fines within the SC units were typically low-plasticity clays. The locations of the investigated buildings and in-situ tests are presented in Figure 1.

3.2 *Liquefaction hazard assessment indices: LPI and LSN*

In geotechnical earthquake engineering, the probability of soil liquefaction induced by strong ground motions has been investigated by various researchers using results from in-situ tests that are frequently employed in practice (Iwasaki et al., 1978; Tonkin & Taylor, 2013). The assessment of liquefaction hazards often extends beyond the simple evaluation of the factor of safety (FS) at discrete depths. To better capture the cumulative effect of liquefaction throughout the soil profile, integrated indices such as the Liquefaction Potential Index (LPI) and Liquefaction Severity Number (LSN) have been developed and widely adopted.

The LPI, first introduced by Iwasaki et al. (1978), combines both the calculated FS and its depth distribution into a single measure, emphasizing liquefaction occurring closer to the ground surface, where damage potential is greater. The index is evaluated down to 20 m depth using:

$$LPI = \int_0^{20} F(z)\, W(z) dz \qquad (4)$$

where *F(z)* is the liquefaction severity function based on the factor of safety (FS) at depth. *F(z)* is equal to "1-*FS(z)*" when *FS(z)<1*. *W(z)* is a depth-weighting term. Based on Iwasaki et al. (1982), LPI values are interpreted as:

- LPI < 5: low liquefaction risk
- 5 ≤ LPI < 15: moderate to high risk
- LPI ≥ 15: very high risk; ground improvement recommended

Despite its broad use, the exclusion of layers with FS > 1 means that soils marginally stronger than the triggering threshold may still be overlooked, even if they can generate excess pore pressures and measurable deformations. In this study, Boulanger & Idriss (2014) approach have used to determine the factor of safety for liquefaction.

The LSN parameter, introduced by Tonkin & Taylor (2013), offers an alternative approach by relating observed surface manifestations directly to liquefaction-induced volumetric strains (ε_v) estimated from CPT or SPT data:

$$LSN = 1000 \int \frac{\varepsilon_v}{z} dz \qquad (4)$$

Volumetric strains are commonly obtained from the strain potential relationships proposed by Zhang et al. (2002), which link ε_v to normalized cone resistance (q_{c1ncs}) and FS. Van Ballegooy et al. (2013) outlined practical thresholds:

- LSN < 20: negligible surface effects, minor sand boils, little or no structural damage
- 20 < LSN < 40: moderate manifestations, some lateral spreading, moderate building damage
- LSN > 40: severe surface rupture, large settlements, significant structural or utility damage

Within the scope of this study, both SPT and CPT data obtained from the field were utilized to calculate internationally recognized liquefaction potential indicators, LPI and LSN. Furthermore, the relationship between these indicators and the potential for structural damage was examined. A design peak ground acceleration (PGA) of 0.25g was adopted for the mainshock scenario, as USGS ShakeMaps and Binici et al. (2023) indicate a PGA of approximately 0.20g for the Gölbaşı district during the Mw 7.8 event. Similarly, Flora et al. (2024) have reported a consistent value of 0.23g based on inverse distance weighting (IDW) interpolation in QGIS using more than 300 strong-motion station records. The adopted value is also consistent with the PGA used by Tonyalı et al. (2024).

3.3 *Settlement and Tilt Prediction Models*

Liquefaction-induced settlements for each building were estimated using three widely adopted methods: Karamitros et al. (2013), Bray & Macedo (2017), and Bullock et al. (2019). The calculated settlements were compared with field measurements to evaluate their predictive performance.

The methods by Karamitros et al. (2013) and Bray & Macedo (2017) require seismic input parameters such as peak ground acceleration (a_{max}), predominant period of the earthquake (T), cumulative absolute velocity (CAV), and standardized cumulative absolute velocity (CAV_{dp}) for estimating liquefaction-induced building settlements. Due to the lack of reliable earthquake records in the Gölbaşı district, caused by power outages and equipment failures, a representative record was selected from the PEER database and synthetic ground motions generated for this study. In contrast, Bullock et al. (2019) incorporates earthquake effects through CAV values derived from fault characteristics, eliminating the need for recorded ground motions.

Karamitros et al. (2013) proposed a simplified analytical method for estimating seismic settlement of strip and rectangular foundations on liquefiable clay soils, based on dynamic numerical analyses with a critical state constitutive model. The approach accounts for punching-type settlement in a clay crust and liquefied sand layers, shear-induced displacements in liquefied substrates, and reduced static safety factors after shaking. The method was validated through centrifuge and large-scale shaking table tests, as well as field observations from the 1999 Kocaeli Earthquake in Adapazarı.

Bray & Macedo (2017) consider total building settlement as the sum of three components: volumetric deformation (D_v). shear-induced settlement (D_s) and deformation due to sand boil material expulsion (D_e). This method proposes a new expression for estimating the shear-induced settlement (D_s) based on statistical analyses of FLAC v7.0 simulations with PM4Sand. The equation provided by the authors requires several inputs including load (q), width of foundations (B), thickness of liquefiable layer (HL), liquefaction building settlement index function (LBS), seismic parameters, CAV_{dp} (cumulative absolute velocity with a threshold of 0.025g) and Sa1 (spectral acceleration with a period of 1 second).

Bullock et al. (2019), developed a probabilistic model for predicting building settlement and tilt based on results from 63000 nonlinear dynamic analyses and centrifuge tests using 3D finite element modeling with PDMY02. Inputs include building geometry and weight, number and thickness of liquefiable layers, and their normalized strengths from SPT or CPT data.

3.4 *Selection and scaling of earthquake records*

The earthquake records used in the calculations were downloaded from the PEER Ground Motion Database (Ancheta et al., 2014). While searching for suitable records, the fault mechanism was selected as lateral strike-slip in accordance with the East Anatolian Fault Zone (EAFZ), and the magnitude of the earthquakes was considered in the range of 7.0-8.0 M_w. Since Gölbaşı district is 80 km away from the epicenter of the earthquake, only the records with R_{jb} distances between 50-100 km were considered. Earthquake records in the range of Vs_{30}=360-500 m/s were filtered to be suitable for the ground profile (Vs_{30}=384 m/s) of TK0203 Gölbaşı station in AFAD's network. As a result of the search in the PEER database, five earthquake records that met the desired characteristics were identified. These records and their characteristics from Puerta LA Cruz, Mecidiyekoy, Maku, Frink and WAKC stations are shown in Table 1.

It is necessary to use the selected earthquake records by scaling (simple scaling) to the largest ground acceleration active in Gölbaşı district. The earthquake records selected from the PEER database for the calculations were scaled to 0.25g PGA by simple scaling method.

In addition to these five recordings, in order to reflect the frequency content of the Kahramanmaras earthquake, a recording station whose ground profile is similar to Gölbaşı station TK0203 in terms of shear wave velocity profile for the first 30 meters and which recorded the main shock at 04.17 am was investigated. As a result of the investigations, it was determined that the dominant frequency in the HVSR graphs of Turkoglu TK4929 station was approximately 1 Hz. This value coincides with the average dominant frequency value measured based on geophysical methods when Gölbaşı TK0203 (AFAD, 2024) station was established. For this reason, the earthquake record of Turkoglu TK4629 station was selected to be used in the calculations and scaled to PGA=0.25g by simple scaling method. The scale factors, CAV (cm/s), Sa (T=1s) and Standardized CAV (g*sec) parameters of the scaled records are as shown in Table 1. All selected and scaled records conform to the strike-slip fault mechanism.

Table 1. Earthquake records selected for use in calculations

Station name	Scale Factor	CAV (cm/s)	Sa (T=1 s)	Standardized CAV (g*sec)
Puerta La Cruz	5.10	2187.15	0.139	2.031
Mecidiyekoy	3.02	902.53	0.136	0.783
Maku	2.72	892.61	0.098	0.790
Frink	6.63	2447.95	0.502	1.811
WAKC	1.65	1831.33	0.441	1.296
Turkoglu (TK4629)	0.72	888.44	0.160	0.872

4 RESULTS

4.1 *LPI – LSN Distributions*

The SPT-based LPI and LSN values, along with the average liquefaction-induced settlements of nearby buildings, are presented in Figure 2. In the figure, blue bars represent LSN values and yellow bars represent LPI values, both referenced to the left vertical axis. The right vertical axis indicates the average building settlement measured in the vicinity of each SPT location, illustrated by open circles. For example, in the vicinity of SPT-1, three buildings were surveyed, exhibiting settlements of 35, 40, and 45 cm; thus, the average settlement for this location was calculated as 40 cm. In the SPT-based assessment, LPI values exceeded 5 at all test locations, indicating that none of the sites can be classified as having a “low” liquefaction risk according to LPI thresholds. This observation is consistent with the documented damage data, which confirm that liquefaction-related effects occurred across the study area.

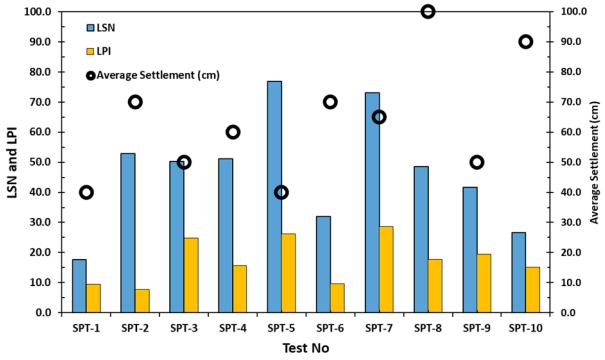

Figure 2. LPI and LSN distributions calculated by SPT based calculation

Only three locations (SPT-1, SPT-2, and SPT-6) yielded LPI values between 5 and 15, corresponding to the "moderate to high risk" range in which moderate levels of damage might be expected. However, in these three locations, the observed building settlements ranged between 40 cm and 70 cm, and all affected buildings became uninhabitable due to excessive tilting. From this perspective, LPI values greater than 15 would have provided a more accurate representation of the actual damage.

In the remaining locations, LPI values exceeded 15, indicating a "very high" liquefaction risk, and these results aligned well with the observed settlements, which ranged between 40 cm and 100 cm. Nevertheless, when comparing the sites with LPI values of 5–15 to those with values above 15, no significant differences were found in the average building settlements. This lack of differentiation suggests that there is no clear linear correlation between LPI values and the magnitude of building settlement in the study area.

For LSN, only one location (SPT-1) yielded a value below 20, which would typically indicate minor or no damage (van Ballegooy et al., 2013). However, the observed average settlement here was about 40 cm, and all buildings became uninhabitable due to excessive tilting, indicating that LSN underestimated the damage. Two sites (SPT-6 and SPT-10) had LSN values between 20 and 40, yet observed settlements were much higher than expected (70–90 cm). At all other locations, LSN values exceeded 40, consistent with severe observed damage. Similar to LPI, no clear correlation was found between LSN and settlement magnitude, likely due to the close spacing and varying heights of buildings, which may have amplified soil–structure interaction effects.

The CPT-based LPI values, calculated using two different soil behavior type index (I_c) cutoff criteria, are presented in Figure 3 together with the average measured settlements of nearby buildings. In the figure, orange bars represent LPI values computed with the conventional $I_c=2.6$ threshold recommended by Boulanger and Idriss (2014), while the yellow bars correspond to recalculated values using a higher cutoff of $I_c=2.8$. The left vertical axis indicates LPI values, and the right vertical axis shows average settlement magnitudes, illustrated by open circles.

When the conventional $I_c=2.6$ threshold was applied, some locations exhibiting substantial liquefaction-induced damage yielded LPI values below 5. For example, CPT-1 and CPT-2, where average settlements of approximately 70 cm were recorded, produced LPI values of less than 5, implying "low liquefaction risk". Given that the Gölbaşı district is predominantly composed of Clayey Sands (SC) and low plasticity clays (CL) (Bozbey et al,. 2023, Çetin et al., 2024), transitional soils with values between 2.6 and 2.8 are common, and these materials can still exhibit significant liquefaction potential. By increasing the cutoff to $I_c=2.8$ LPI values increased in several locations, improving the alignment with observed damage patterns. Notable changes were observed in CPT-6, where LPI rose from 10 to 15, and in CPT-3, where LPI increased from 15 to 19. The latter site exhibited an average settlement of about 100 cm, and the higher cutoff provided a more realistic reflection of the severe damage observed. However, in CPT-1 and CPT-2, LPI values remained below 5 even after the adjustment, indicating that the method continued to underestimate the risk in these areas.

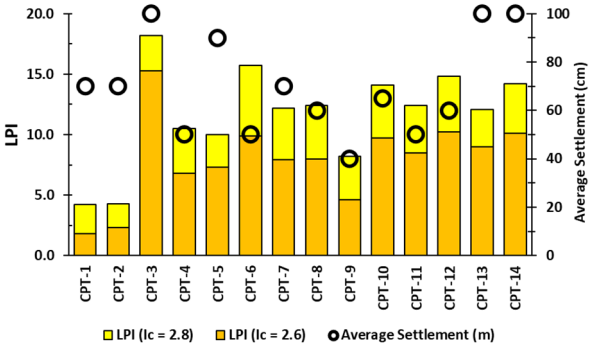

Figure 3. LPI distributions and observed mean settlement by CPT based calculation

For LSN, the CPT-based results showed a similar trend to those observed for LPI as shown in Figure 4. At several locations, specifically CPT-1, CPT-2, CPT-5, CPT-9, and CPT-13, the index underestimated the severity of damage regardless of whether an *Ic* cutoff of 2.6 or 2.8 was applied. In these areas, the calculated LSN values suggested lower levels of liquefaction effects, yet the measured average settlements ranged between 70 cm and 100 cm, and the observed building damage was severe.

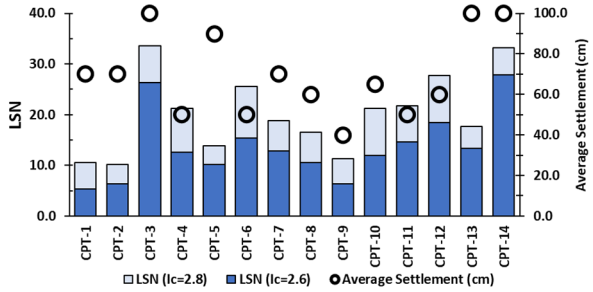

Figure 4. LSN distribution and observed mean settlement by CPT based calculation

In all other CPT locations, LSN values ranged between 20 and 40, corresponding to "moderate" liquefaction effects and an expectation of average building damage. However, the observed damage in these areas was far more significant: all affected buildings were rendered unusable due to excessive settlement and tilting. Increasing the I_c cutoff from 2.6 to 2.8 did not raise the LSN values above 40 in these cases. Therefore, for CPT-based calculations, both the LPI and LSN indices tended to underpredict the severity of liquefaction-induced damage observed in the study area.

4.2 *Comparison of measured settlements with prediction methods*

The correlation graph between the settlement values estimated using the method of Karamitros et al. (2013) and the measured settlement values is shown in Figure 5. As can be seen, the calculated settlement values are considerably lower than the measured settlements. The correlation coefficient (R^2) between the calculated and measured settlements was 0.08. This method

was not able to accurately predict the settlements that occurred in any of the buildings during the earthquake. The reason for this large difference between the predictions and the observations may be that the actual effect of the earthquake is larger than the coefficients a_{max}, T and N considered in the calculations. Another reason may be that the method misestimates the reduced bearing capacity safety factor when estimating liquefaction-induced building settlements. Previous studies investigating the success of this method have found that the method underestimates the actual liquefaction-induced building settlements (Quintero et al., 2018).

An Excel worksheet developed by the authors was used to calculate building settlements using the Bray & Macedo (2017) method. In the worksheet, shear-induced settlements are calculated automatically by entering the parameters Sa1, CAV_{dp}, B, HL (liquefied layer thickness), Q (building weight) and LBS (Liquefaction Building Settlement Index). The correlation graph between the settlement values estimated by this method and the measured settlement values is shown in Figure 6. This method, like Karamitros et al. (2013), underestimated the measured building settlements in the field. The correlation coefficient (R^2) between predicted settlements and measured settlements was calculated as 0.10.

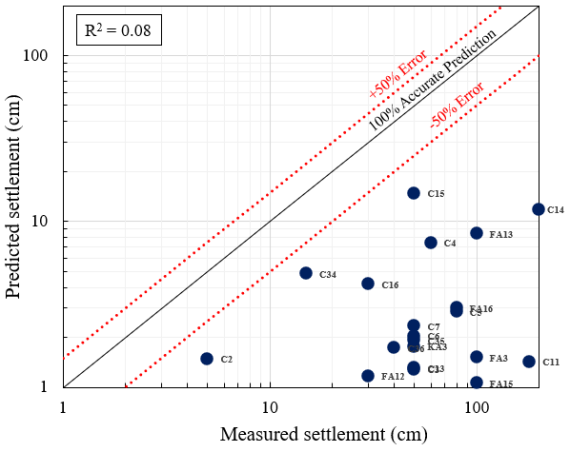

Figure 5. Correlation between measured settlement values and settlement values estimated using the method of Karamitros et al. (2013).

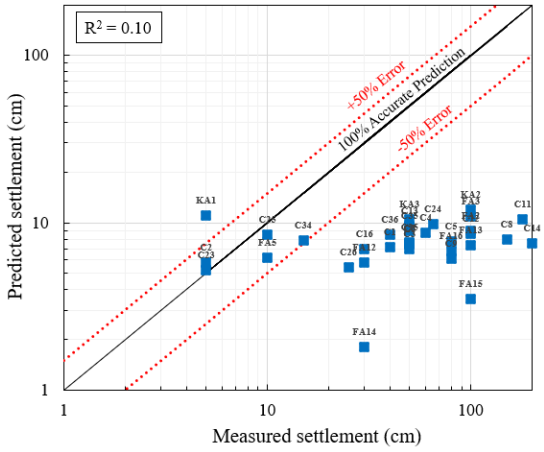

Figure 6. Correlation between measured settlement values and settlement values estimated using the method of Bray & Macedo (2017).

An Excel worksheet developed by the authors was used to calculate building settlements using the Bullock et al. (2019) method. After defining the characteristics of the fault that will produce the earthquake (M_w, fault type, distance to the fault, fault depth), building characteristics (number of storeys, L, B, building weight) and soil characteristics (liquefiable layer characteristics, non-liquefiable crustal layer characteristics) in the worksheet, settlements due to liquefaction are calculated automatically. The effect of the earthquake is included in the calculations with the CAV_{dp} parameter. This parameter is calculated probabilistically considering the characteristics of the fault and the seismicity of the region. In this study, while calculating the CAV_{dp} parameter, shallow and laterally thrust fault characteristics were selected and the parameters M_w=7.8, R_{rup}=1 km, focal depth=10 km were used. The correlation graph between the estimated settlement values and measured settlement values of the buildings with this method is shown in Figure 7 and the correlation graph between the estimated rotation values and measured rotation values is shown in Figure 8. The correlation coefficient (R^2) between the estimated and measured settlements was calculated as 0.13, while the correlation coefficient (R^2) between the estimated and measured tilts was found to be 0.08. Unlike the other two methods, it can be said that this method captures settlements in some buildings in the study areas. A similar situation is observed in the tilts predictions.

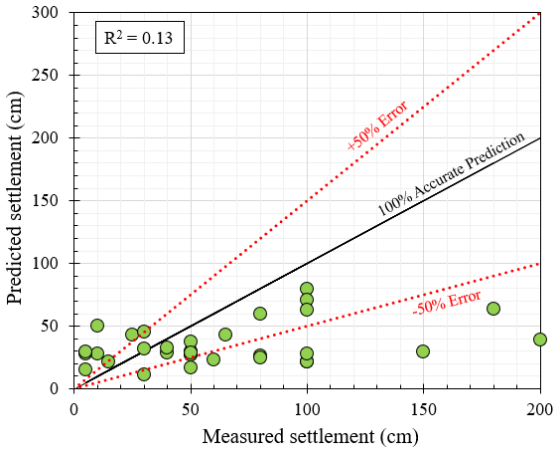

Figure 7. Correlation between measured settlement values and settlement values estimated using the method of Bullock et al. (2019).

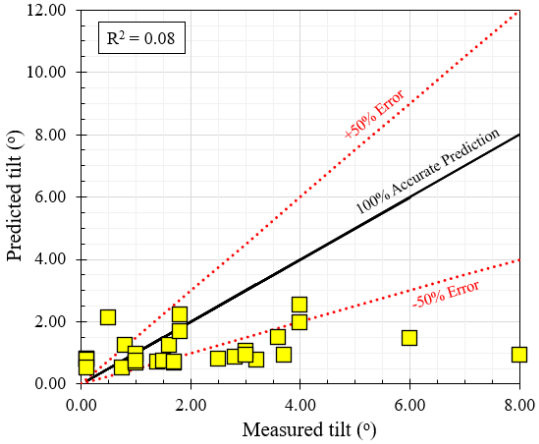

Figure 8. Correlation between measured tilt values and tilt values estimated using the method of Bullock et al. (2019).

When all methods are evaluated, Karamitros et al. (2013) and Bray & Macedo (2017) methods tend to underestimate settlements. Although the Bullock et al. (2019) method closely predicted the settlements in some buildings, it did not perform well in the 34 buildings predicted in general.

5 CONCLUSION

This study evaluated the predictive accuracy of existing liquefaction-induced damage assessment methods by comparing them with measured settlement and tilt data from 34 buildings affected by the 6 February 2023 Kahramanmaraş earthquakes in the Gölbaşı district of Adıyaman province. Field investigations included Standard Penetration Tests (SPT) and Cone Penetration Tests (CPT) near the surveyed buildings.

The Liquefaction Potential Index (LPI) and Liquefaction Severity Number (LSN) were calculated from both SPT and CPT data, while foundation settlements were estimated using the empirical models of Karamitros et al. (2013), Bray & Macedo (2017), and Bullock et al. (2019). Among these, the Karamitros and Bray & Macedo methods generally underestimated settlements, whereas the Bullock method performed better for some cases but did not achieve consistent accuracy across all sites.

Comparisons revealed that LPI and LSN values derived from SPT data aligned more closely with the observed damage than those from CPT data. This suggests that in areas dominated by transitional soils, conventional CPT-based liquefaction indices may not be able to estimate the damage severity.

Overall, the findings highlight the limitations of widely used liquefaction hazard indices and settlement prediction models, emphasizing the need for site-specific calibration, particularly for deep alluvial deposits with pronounced stratification and interbedded clay–sand layers.

6 ACKNOWLEDGEMENTS

This study was carried out within the scope of the project titled "*Development of an analytical approach for the prediction of liquefaction-induced foundation damage in shallow-foundation buildings on silty-clay alluvium soils considering building characteristics and neighboring building interaction: Adıyaman–Gölbaşı Case*" (Project No: 123M604), supported by the Scientific and Technological Research Council of Türkiye (TÜBİTAK). The authors gratefully acknowledge the support provided by TÜBİTAK. Special thanks are also extended to Zemin Etüd A.Ş. for conducting the field tests.

7 REFERENCES

AFAD, 2024. AFAD TADAS station list [Web document]. Avaible at: https://tadas.afad.gov.tr/list-station [Accessed 12th August 2024].

Ancheta, T.D., Darragh, R.B., Stewart, J.P., Seyhan, E., Silva, W.J., Chiou, B.S.-J., Wooddell, K.E., Graves, R.W., Kottke, A.R., Boore, D.M., Kishida, T. and Donahue, J.L. 2014. NGA-West2 database. *Earthquake Spectra* 30(3), 989-1005. https://doi.org/10.1193/070913EQS197M.

Binici, B., Yakut, A., Canbay, E., Demirel, I.O., Kahraman, M., Erberik, A., Yaman, I. O., Baran, E., Canbolat, A., Kadas¸ K., Oztaskin, O., Aktas¸ S., 2023. Performance of Residential Structures. In: Çetin, K. O., Ilgaç, M., Can, G., Çakır, E. (Eds.), Preliminary Reconnaissance Report on February 6, 2023, Pazarcık Mw=7.7 and Elbistan Mw=7.6, Kahramanmaras¸-Türkiye Earthquakes Report no: METU/EERC 2023–01. Middle East Technical University, Earthquake Engineering Research Center, Ankara,pp. 43–51.

Boulanger, R.W. and Idriss, I.M., 2014. CPT and SPT Based Liquefaction Triggering Procedures. Report No. UCD/CGM-14/01. Davis, CA: University of California.

Bozbey, I. et al., 2023. Development of an analytical approach for the prediction of liquefaction-induced foundation damage in shallow-foundation buildings on silty-clay alluvium soils considering building characteristics and neighboring building interaction Adıyaman-Gölbaşı Case, Ankara: TUBİTAK.

Bozbey, I., Keleşoğlu, M. K., Öztoprak, S., Altınok, E., Sargin, S., Öser, C., ... & Tütüncü, Y. E., 2024. Adiyaman Gölbaşi alüvyon havzasindaki yüzeysel temelli binalarda 6 Şubat 2023 depremlerinde oluşan deformasyonlarin incelenmesi. Zemin Mekaniği ve Geoteknik Mühendisliği 19. Ulusal Konferansı. Ankara, 17-18 Ekim 2024.

Bray, J. D., Sancio, R. B., Durgunoglu, T., Onalp, A., Youd, T. L., Stewart, J. P. ,...& Karadayilar, T. 2004. Subsurface characterization at ground failure sites in Adapazari, Turkey. *Journal of Geotechnical and Geoenvironmental Engineering*, *130*(7), 673-685. https://doi.org/10.1061/(ASCE)1090-0241(2004)130:7(673)

Bray, J.D. and Macedo, J. 2017. 6th Ishihara lecture: Simplified procedure for estimating liquefaction-induced building settlement. *Soil Dynamics and Earthquake Engineering* 102, 215-231. https://doi.org/10.1016/j.soildyn.2017.08.026.

Bray, J.D. and Stewart, J.P. 2000. Damage patterns and foundation performance in Adapazari, Kocaeli Turkey earthquake of August 17, 1999. Reconnaissance Report, *Earthquake Spectra* 16, 163-189.

Bullock, Z., Dashti, S., Karimi, Z., Liel, A., Porter, K. and Franke, K. 2019. Probabilistic Models for residual and peak transient tilt of mat-founded structures on liquefiable soils. *Journal of Geotechnical and Geoenvironmental Engineering* 145(2). https://doi.org/10.1061/(ASCE)GT.1943-5606.0002002.

Cetin, K. O., Moug, D., Soylemez, B., Ayhan, B. U., Zarzour, M., Suhaily, A. A., ... & Duman, E. 2025. Ground failures and foundation performances in Adıyaman–Gölbaşı following the 6 February 2023 Kahramanmaraş–Türkiye earthquake sequence. *Earthquake Spectra, 41*(1), 249-289.

Flora, A., Bilotta, E., Valtucci, F., Fierro, T., Perez, R., Santucci de Magistris, F., Modoni, G., Spacagna, R., Kelesoglu, M.K., Sargin, S., Altinok, E., Oztoprak, S., Bozbey, I. and Aysal, N. 2024. Liquefaction effects in the city of Gölbaşı: from the analysis of predisposing factors to damage survey. *Engineering Geology* 338, 107633. https://doi.org/10.1016/j.enggeo.2024.107633.

Iwasaki, T., Tatsuoka, F., Tokida, K. and Yasuda, S. 1978. A practical method for assessing soil liquefaction potential based on case studies at various sites in Japan. *In: Proc. of 2nd Int. National Conf. On Microzonation*, pp. 885–896.

Karamitros, D.K., Bouckovalas, G.D. and Chaloulos, Y.K. 2013. Seismic settlements of shallow foundations on liquefiable soil with a clay crust. *Soil Dynamics and Earthquake Engineering* 46, 64-76. https://doi.org/10.1016/j.soildyn.2012.11.012.

Moug, D., Bassal, P., Bray, J.D., Cetin, K.O., Kendir, S.B., Sahin, A., Çakır, E., Söylemez, B. and Ocak, S. 2023. February 6, 2023 Türkiye earthquakes: GEER phase 3 team report on selected geotechnical engineering effects. *Geotechnical Extreme Events Reconnaissance (GEER) Association*, Report No. GEER-082-S1, 30. https://doi.org/10.18118/G6F379.

Quintero, J., Saldanha, S., Millen, M., Fonseca, A.V.D., Sargin, S., Oztoprak, S. and Kelesoglu, M.K. 2018. Investigation into the settlement of a case study building on liquefiable soil in Adapazari, Turkey. *In Geotechnical Earthquake Engineering and Soil Dynamics V*, 321-336. Reston, VA: American Society of Civil Engineers. https://doi.org/10.1061/9780784481455.032.

Tonkin & Taylor Ltd. 2013. Liquefaction vulnerability study. *Report prepared for the Earthquake Commission (EQC)*. New Zealand. Retrieved from https://www.eqc.govt.nz.

Tonyalı, İ., Akbas, S.O., Beyaz, T., Kayabalı, K. and Gokceoglu, C. 2024. Case study of a foundation failure induced by cyclic softening of clay during the 2023 Kahramanmaraş earthquakes. *Engineering Geology* 332, 107477, ISSN 0013-7952.

Van Ballegooy, S., Lacrosse, V., Jacka, M. and Malan, P., 2013. LSN–a new methodology for characterising the effects of liquefaction in terms of relative land damage severity. In: Chin, C.Y., ed., Proceedings of the 19th NZGS Geotechnical Symposium. Queenstown, 21-24 November 2013.

Zhang, G., Robertson, P.K. and Brachman, R.W., 2002. Estimating liquefaction-induced ground settlement from CPT for level ground. Canadian Geotechnical Journal, 39(5), pp.1168-1180

Iwasaki, T., Arakawa, T. and Tokida, K., 1982. Simplified procedures for assessing soil liquefaction during earthquakes. In: Proceedings of the Conference on Soil Dynamics and Earthquake Engineering. Southampton, 13-15 July 1982. pp.925-939.